ORIGINAL PAPER

Nagoya J. Med. Sci. **85**. 772–778, 2023
doi:10.18999/nagjms.85.4.772

Microglial process dynamics depend on astrocyte and synaptic activity

Ako Ikegami, Daisuke Kato and Hiroaki Wake

Department of Anatomy and Molecular Cell Biology, Nagoya University Graduate School of Medicine, Nagoya, Japan

ABSTRACT

Microglial processes survey the brain parenchyma, but it is unknown whether this process is influenced by the cell activity of nearby microglia under physiological conditions. Herein, we showed that microglial process dynamics differ when facilitated by astrocytic activity and pre-synaptic activity. The results revealed distinct microglial process dynamics associated with the activity of other brain cells.

Keywords: microglia, neural activity, astrocyte, spine, synapse

Abbreviations:
eGFP: enhanced green fluorescent protein
ROI: region of interest

INTRODUCTION

Microglia are sensitive brain immune cells that detect and respond to any changes in the central nervous system.[1,2] They are evenly distributed throughout the brain and have ramified processes that constantly extend and retract as they survey almost all elements of neural circuits—neuronal somata, synapses, dendrites, axons, and extracellular matrices.[3-5] Although such brain sampling enables rapid detection and response to neuronal damage,[4,6,7] increasing evidence points to a more nuanced role in brain homeostasis beyond mere immunosurveillance. The physical characteristics and molecular mechanisms of microglial movement are complex. Microglial process movements can range from targeted chemotaxis toward neuronal damage to parenchymal surveillance by microglial processes and fine filopodia that extend from these process ends.[5,8,9] If microglial processes distinctly detect and/or contribute to synaptic plasticity, synapse formation, and elimination, it can be hypothesized that the activity of nearby cells affects their movement trajectories and dynamics. To test this hypothesis, we used two-photon

Received: December 6, 2022; accepted: January 4, 2023
Corresponding Authors: Ako Ikegami, MSc; Hiroaki Wake, MD, PhD
Department of Anatomy and Molecular Cell Biology, Nagoya University Graduate School of Medicine, 65 Tsurumai-cho, Showa-ku, Nagoya 466-8550, Japan (Ikegami, Wake)
Tel: +81-52-744-2004 (Ikegami, Wake), Fax: +81-52-744-2011 (Ikegami, Wake),
E-mail: a-ike@med.nagoya-u.ac.jp (Ikegami); hirowake@med.nagoya-u.ac.jp (Wake)

in vivo imaging of microglia and apical dendrites in the primary motor cortex of CX3CR1$^{\text{enhanced green fluorescent protein (eGFP)/+}}$ mice[10] to simultaneously visualize microglia, astrocytes, and pre-synaptic and post-synaptic activity.

MATERIALS AND METHODS

Animals

All animal experiments were approved by the Animal Care and Use Committees of Nagoya University and Kobe University. All mice were 10–14 weeks old males and had free access to food and water and were kept on a 12 h light/dark cycle. To image microglia, we used CX3CR1$^{\text{eGFP/+}}$ mice, which express eGFP under the control of the *Cx3cr1* promoter.[10]

Surgery and adeno-associated virus injection

To image microglia in vivo, we first attached a custom-made imaging head plate to mice anesthetized with ketamine (74 mg/kg, ip) and xylazine (10 mg/kg, ip). The skin was disinfected with 70% (w/v) ethanol, the skull was exposed and cleaned, and the head plate was firmly attached to dental cement (G-CEM ONE; GC, Tokyo, Japan). After 1 day of recovery, we performed a craniotomy with or without viral injection. Under isoflurane (1%) anesthesia, a circular hole (diameter, 2 mm) was opened over the left primary motor cortex (centered 0.2 mm anterior and 1 mm lateral to the bregma). Next, layer 1 of the primary motor cortex was injected with AAV8-GfaABC1D-GCaMP6s-P2A-mRuby (6.19×10^{11} vector genomes/ml) to visualize the Ca^{2+} activity of astrocytes and AAV1-hSyn-GCaMP6s-P2A-mRuby (Addgene; 8.29×10^{12} vector genomes/ml) to visualize the post-synapses. The latter virus was infused into the ventral lateral nucleus of the thalamus to view the thalamocortical axon terminals of the primary motor cortex and study the pre-synapses. In each case, 0.5 μL of virus cocktail was injected through a glass pipette (tip diameter, 30 μm; GDC-1, Narishige, Tokyo, Japan) for 5 min (IM-300; Narishige, Tokyo, Japan) and left in place for another 5 min before withdrawal. An Agarose L (Nippon Gene, Tokyo, Japan) solution (2% w/v) was then poured over the exposed brain surface and a glass window comprising two coverslips (Matsunami Glass, Osaka, Japan) sealed with an ultraviolet curable adhesive (NOR-61, Norland) was implanted over the craniotomy. The edges of the cranial window were sealed with dental cement and adhesive resin cement (FUJI LUTE BC; GC, Tokyo, Japan; Super Bond; Sun Medical, Shiga, Japan).

Two-photon imaging

We used a laser scanning system (NIS-Elements; Nikon Instech Co, Ltd, Tokyo, Japan) and a mode-locked Ti: sapphire Chameleon Ultra II laser (Coherent, Santa Clara, CA) tuned to 950 nm with a water-immersion objective lens (×25, NA 1.10; Nikon Instech Co, Ltd).

Fluorescence was separated by a 560 nm dichroic mirror with 500–550 nm (green channel: for eGFP fluorescence detection) and a 593 nm mirror with 601–657 nm (red channel: for tdTomato fluorescence detection) emission filters. The laser intensity was 3.5–15 mW.

All imaging sessions were conducted in the primary motor cortex of awake mice at a depth of 50–100 μm below the cortical surface. In imaging sessions to quantify Ca^{2+} activity of astrocytes and pre/post-synapses, continuous 2,000-frame images (173.11 μm × 173.11 μm imaging field with a pixel size of 0.338 μm and a resolution of 512×512 pixels) were captured at a 2-frame/s scanning rate.

Image analysis

In vivo images were analyzed using the ImageJ plug-in (1.37v; NIH) and programs written in MATLAB (version 8; MathWorks). Images were corrected for focal/XY plane displacements using StackReg and TurboReg and open-source code for 3D two-photon imaging registration (available at https://github.com/atakehiro/TurboReg_macro). Astrocytic and pre-/post-synaptic Ca^{2+} activity were integrated as the area under the curve (AUC) of $\Delta F/F_0$ GCaMP values within the region of interest (ROI) using a custom-made MATLAB code. For astrocytes, ROIs were determined using Astrocyte Quantitative Analysis software (AQuA, MATLAB version).[11] Pre-/post-synaptic ROIs were determined using the Wand Tool in ImageJ. In both cases, ROIs with eGFP $\Delta F/F_0$ values greater than 7 or a single AUC duration longer than 60 frames (2-frame/s) were excluded from the analysis to avoid signal contamination by microglial eGFP fluorescence. Likewise, the microglial summed intensity over 2,000 frames (2-frame/s) was calculated within a doughnut-shaped region around each Ca^{2+} signal ROI to exclude GCaMP fluorescence. Microglial process movement was tracked using the Manual Tracking Tool in ImageJ, as described above, and four specific XY positions were extracted for further analysis: 1) the microglial process tip position at the first imaging frame (A); 2) the centroid of each ROI (B); 3) the microglial process tip position at frame t where the distance between A and B was the smallest during the session (P: ie, the microglial process tip located closest to the ROI); and 4) a perpendicular line from point X to a line segment AB (X). Using these values, the length of the line segment AX was defined as the "vector length" and calculated as follows:

$$\mathrm{cosA} = \frac{|\mathrm{AX}|}{|\mathrm{AP}|}$$

$$|\mathrm{AX}| = |\mathrm{AP}|\mathrm{cosA}$$

$$AP\_\_AB = |AP|v\_|AB|v\_cosA$$

$$|\mathrm{AX}| = \frac{AP\_\_AB}{|AB|v\_cosA}$$

Statistics

Pearson's correlation and regression analyses were performed to test for statistical significance using MATLAB and GraphPad Prism v7.0a. $P < 0.05$ was considered significant.

RESULTS

Since distinct microglial process movements are associated with spine formation and elimination, we investigated possible synaptic signals that could influence microglial process dynamics. Adenosine 5'-triphosphate (ATP) is a well-known attractant of microglial processes,[4] while astrocytes are a major source of ATP in the brain.[12] Other neurotransmitters, released from pre-synaptic terminals or released as glio-transmitters, can also evoke responses in microglia and/or modulate process dynamics.[12-14] Therefore, we imaged activity in different cellular compartments associated with synapses together with microglial process dynamics. The calcium indicator, GCaMP6f, was expressed in astrocytes, post-synaptic pyramidal neurons in the primary motor cortex, or pre-synaptic terminals of the thalamic afferent to the primary motor cortex in different cohorts of $CX3CR1^{eGFP/+}$ mice (Fig. 1A and 1B). Ca^{2+} activity in these cellular components was integrated (AUC) and plotted against the parameters of the microglial process tip movements.

Tip motility was tracked and quantified by measuring the velocity and "vector length," ie, the distance that a microglial process tip traveled toward each cellular target ROI from its initial position (Fig. 1A and 1B, see also Methods). The plots of Ca^{2+} activity against the parameters of process motility were fitted to the regression lines to examine the correlations. Astrocytic Ca^{2+} activity was negatively correlated with microglial velocity and weakly positively correlated with vector length (Fig. 1C). Around active astrocytes, their stronger activity attracts the microglial process tips, slowing their velocity. Pre-synaptic Ca^{2+} activity was also weakly negatively correlated with the microglial velocity and strongly correlated with vector length compared to astrocytes (Fig. 1D). Again, we interpret this as the more active a pre-synaptic terminal is, the more it attracts microglia; however, active nerve terminals are also associated with slower tip motility. In contrast, there were no significant correlations between post-synaptic or dendritic Ca^{2+} activity and microglial velocity or vector length (Fig. 1E and 1F). We further quantified Ca^{2+} activity in single spines (Fig. 1G). Consistent with this, reflecting local input from pre-synaptic terminals,[15] we again found a weak positive correlation between single spine Ca^{2+} activity and microglial vector length (Fig. 1G). The reduced tip velocity associated with activity in astrocytes

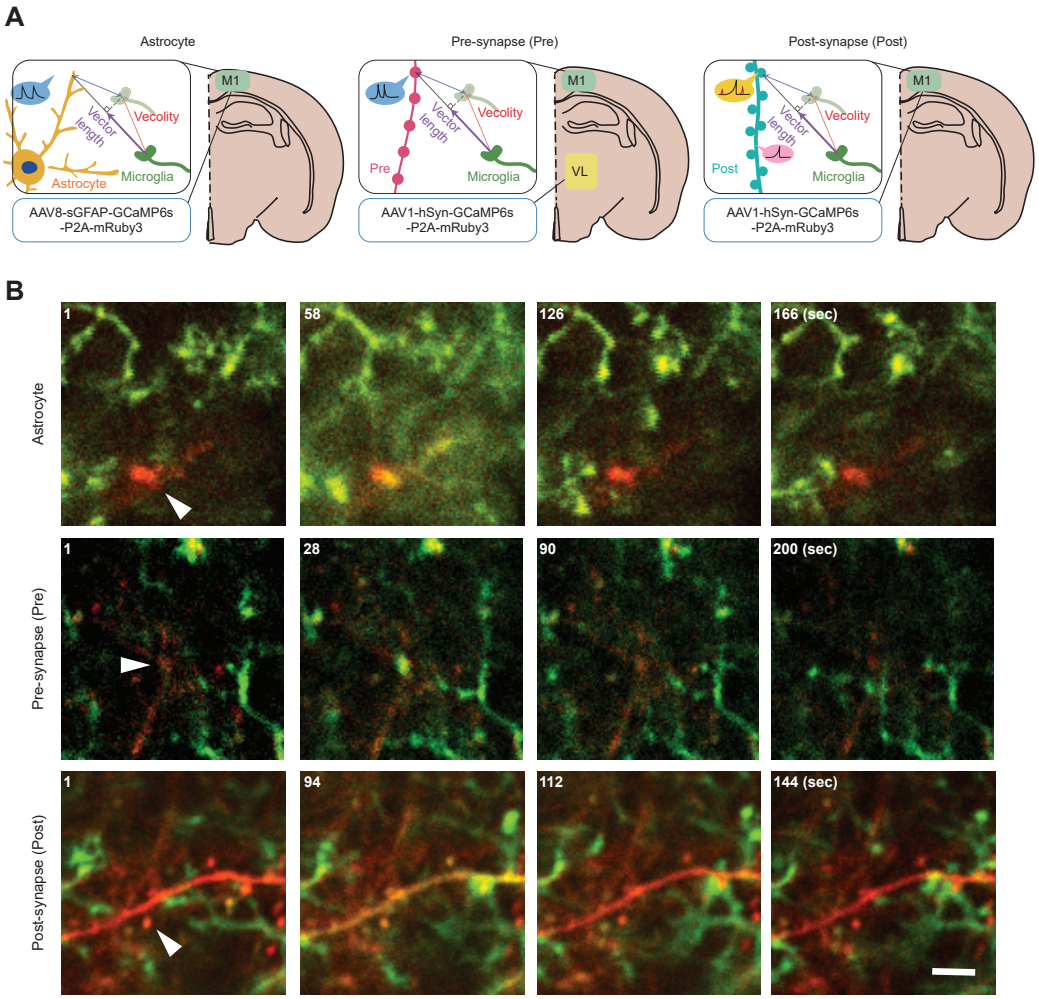

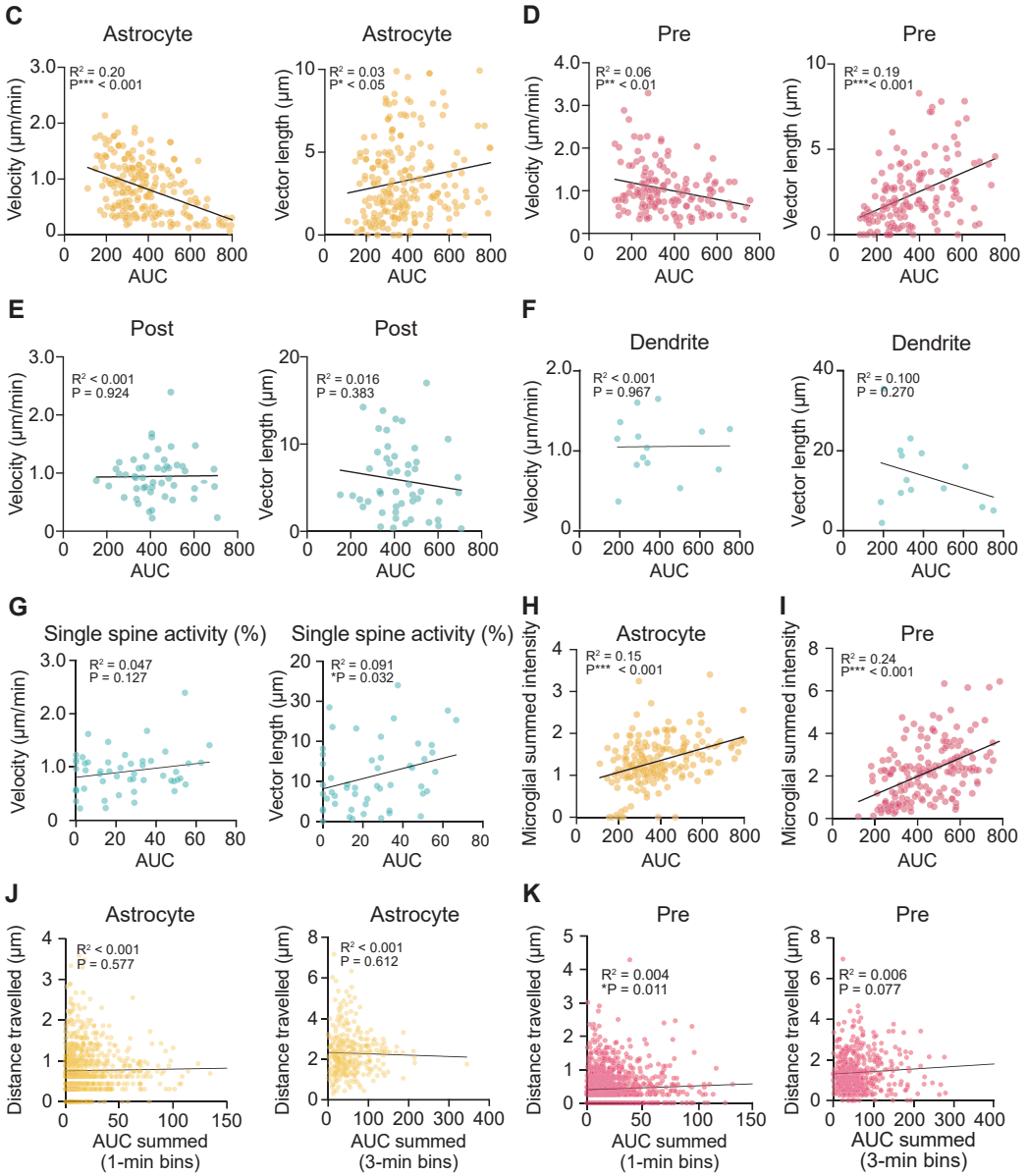

Fig. 1 Ca^{2+} activity of astrocytes and pre-synapses affects microglial process movement in different ways
A, Schematic diagram showing the imaging of Ca^{2+} transients (blue transients) in astrocytes (n = 6 mice) and pre-synapses (n = 6 mice) and Ca^{2+} transients in post-synapses (dendrites [pink balloon] and spines [single spine activity indicated by the red plot in yellow balloons], n = 5 mice), while simultaneously measuring microglial movement velocity and vector length. Post-synapse data, relevant adeno-associated virus vectors, and injection sites are also shown. **B**, Representative image frames showing different interactions between microglial process tips (green) and other cellular elements (astrocyte, pre-synapse, post-synapse: red), with their Ca^{2+} activities (green + red = yellow) indicated in the second panel from left. Scale bar = 5 μm. **C, D and E**, Ca^{2+} activity was integrated (AUC) and plotted against microglial process velocity and displacement for astrocytes (C), pre-synapse (D), and post-synapse (E). The plots fit linear regression. **F and G**, Scatter plots of dendritic (F) or single spine (G) Ca^{2+} activity integrals against the velocity (left) and vector length (right) of microglial process movement. The lines show fit to the data with a simple linear regression. **H and I**, Ca^{2+} activity in astrocytes (H) and pre-synapses

(I) are plotted against microglial astrocytes or pre-synapse interaction intensity. **J**, The plot of astrocyte Ca^{2+} activity integrals binned into 1- and 3-min time intervals (for 2,000-frame imaging of approximately 17 min) and microglial distance traveled during each bin. No correlation is observed, indicating that no time-dependent astrocytic component attracted microglial movements. **K**, The plot of the integral of pre-synaptic Ca^{2+} activity binned into 1- and 3-min time intervals and microglial distance traveled during each bin. A significant but weak positive correlation was observed with the 1-min AUC bins, suggesting larger but less sustained Ca^{2+} transients were associated with microglial movements. Slopes of regression lines in (C–K) were compared to a slope of 0 using simple linear regression; p values are shown in the graphs.

AUC: area under the curve
M1: primary motor cortex
VL: ventral lateral nucleus

and pre-synapses suggests that microglial processes may be pausing and contacting synaptic elements. To probe the characteristics of these possible interactions, we quantified the parameters of repetitive microglial movements by measuring the intensity of the summed interaction. The astrocytic activity was weakly positively correlated and pre-synaptic activity was positively correlated with summed microglial intensity (Fig. 1H and 1I). Finally, we examined whether vector length correlated with AUC when we measured astrocytic and pre-synaptic activity over a reduced time window (Fig. 1J). The astrocyte correlations were lost, indicating that the summed activity was only associated with the attraction of microglial processes. In contrast, we observed a correlation (albeit weaker) between pre-synapse activity in 1 min bins and microglial distance traveled (Fig. 1K). This pattern was consistent with a more repetitive attraction to pre-synapses over a brief timeframe.

DISCUSSION

Through concurrent imaging of microglia, neurons, and astrocytes, we showed that astrocytic and pre-synaptic activity changes the microglial process dynamics. Microglial processes made random but prolonged contact with dendrites at sites where new spines later appeared. We revealed a key role for astrocyte activity and subsequent vesicular release in supporting microglial process dynamics that promote dendrite interactions that lead to spine formation and elimination. We occasionally observed the acute appearance of filopodia at dendrite contact sites, as observed during development in the somatosensory cortex.[16] Since microglial attraction by astrocytic activity and pre-synaptic activity was due to some substance released from astrocytes or pre-synapse, the distance from astrocytes or pre-synapse to microglia influences these attractions. Previous studies have shown that ATP-induced microglial attraction depends on the concentration of ATP. We further need to investigate the geometric arrangement of the astrocyte process and the pre-synapse with the microglia process.

AUTHOR CONTRIBUTIONS

A.I. and H.W. designed the research; A.I., D.K. and H.W. performed the research and analyzed data; A.I. and H.W. wrote the paper.

ACKNOWLEDGEMENTS

We thank T. Furuyashiki (Kobe University) for sharing CX3CR1$^{eGFP/+}$ mice. This work was supported by Grants-in-Aid for Scientific Research on Innovative Areas (15H01300, 16H01346, 17H05747, 19H04753, 19H05219 and 25110732 to H.W.).

CONFLICTS OF INTEREST

The authors declare no competing interests.

REFERENCES

1 Hanisch UK, Kettenmann H. Microglia: active sensor and versatile effector cells in the normal and pathologic brain. *Nat Neurosci.* 2007;10(11):1387–1394. doi:10.1038/nn1997.
2 Kettenmann H, Kirchhoff F, Verkhratsky A. Microglia: new roles for the synaptic stripper. *Neuron.* 2013;77(1):10–18. doi:10.1016/j.neuron.2012.12.023.
3 Cserép C, Pósfai B, Lénárt N, et al. Microglia monitor and protect neuronal function through specialized somatic purinergic junctions. *Science.* 2020;367(6477):528–537. doi:10.1126/science.aax6752.
4 Davalos D, Grutzendler J, Yang G, et al. ATP mediates rapid microglial response to local brain injury in vivo. *Nat Neurosci.* 2005;8(6):752–758. doi:10.1038/nn1472.
5 Nimmerjahn A, Kirchhoff F, Helmchen F. Resting microglial cells are highly dynamic surveillants of brain parenchyma in vivo. *Science.* 2005;308(5726):1314–1318. doi:10.1126/science.1110647.
6 Haynes SE, Hollopeter G, Yang G, et al. The P2Y12 receptor regulates microglial activation by extracellular nucleotides. *Nat Neurosci.* 2006;9(12):1512–1519. doi:10.1038/nn1805.
7 Hines DJ, Hines RM, Mulligan SJ, Macvicar BA. Microglia processes block the spread of damage in the brain and require functional chloride channels. *Glia.* 2009;57(15):1610–1618. doi:10.1002/glia.20874.
8 Bernier LP, Bohlen CJ, York EM, et al. Nanoscale Surveillance of the Brain by Microglia via cAMP-Regulated Filopodia. *Cell Rep.* 2019;27(10):2895–2908.e4. doi:10.1016/j.celrep.2019.05.010.
9 Smolders SM, Kessels S, Vangansewinkel T, Rigo JM, Legendre P, Brône B. Microglia: Brain cells on the move. *Prog Neurobiol.* 2019;178:101612. doi:10.1016/j.pneurobio.2019.04.001.
10 Jung S, Aliberti J, Graemmel P, et al. Analysis of fractalkine receptor CX(3)CR1 function by targeted deletion and green fluorescent protein reporter gene insertion. *Mol Cell Biol.* 2000;20(11):4106–4114. doi:10.1128/MCB.20.11.4106-4114.2000.
11 Wang Y, DelRosso NV, Vaidyanathan TV, et al. Accurate quantification of astrocyte and neurotransmitter fluorescence dynamics for single-cell and population-level physiology. *Nat Neurosci.* 2019;22(11):1936–1944. doi:10.1038/s41593-019-0492-2.
12 Lalo U, Palygin O, Verkhratsky A, Grant SG, Pankratov Y. ATP from synaptic terminals and astrocytes regulates NMDA receptors and synaptic plasticity through PSD-95 multi-protein complex. *Sci Rep.* 2016;6:33609. doi:10.1038/srep33609.
13 Liu YU, Ying Y, Li Y, et al. Neuronal network activity controls microglial process surveillance in awake mice via norepinephrine signaling. *Nat Neurosci.* 2019;22(11):1771–1781. doi:10.1038/s41593-019-0511-3.
14 Stowell RD, Sipe GO, Dawes RP, et al. Noradrenergic signaling in the wakeful state inhibits microglial surveillance and synaptic plasticity in the mouse visual cortex. *Nat Neurosci.* 2019;22(11):1782–1792. doi:10.1038/s41593-019-0514-0.
15 Araya R, Vogels TP, Yuste R. Activity-dependent dendritic spine neck changes are correlated with synaptic strength. *Proc Natl Acad Sci U S A.* 2014;111(28):E2895-E2904. doi:10.1073/pnas.1321869111.
16 Miyamoto A, Wake H, Ishikawa AW, et al. Microglia contact induces synapse formation in developing somatosensory cortex. *Nat Commun.* 2016;7:12540. doi:10.1038/ncomms12540.